MASTER OF PHILOSOPHY Modelling of Materials

Examiner's Solutions to Paper 2

SECTION A

1(a)

Nucleation is the process by which a new phase first appears in a first-order phase transformation. Homogeneous nucleation occurs by natural (thermodynamic equilibrium) fluctuations in the parent phase. Heterogeneous nucleation occurs on catalytic substrates of a foreign phase embedded in the parent phase.

In homogeneous nucleation, there are three main input parameters in calculating the nucleation rate: the number of molecules per unit volume, the free energy difference between parent and new phases, and the interfacial energy between the parent and new phases. Of these, the first two are usually well known, but interfacial energy is not well known (either from experiment or from calculation). Indeed the interfacial energy is often estimated from measurement of nucleation rate. Unfortunately, the nucleation rate is extremely sensitive to the value of interfacial energy (as the interfacial energy appears to the third power in the argument of an exponential in the expression for nucleation rate).

The uncertainty about interfacial energies is an even worse problem for heterogeneous nucleation. In this case, the rate is very dependent on the contact angle of the nucleating phase on the substrate. The contact angle depends on the relative magnitudes of the three interfacial energies in the problem (between parent phase and new phase, between parent phase and substrate, and between new phase and substrate). None of these energies is well known and therefore the crucial contact angle is not well known. Furthermore, in heterogeneous nucleation there is likely to be spectrum of heterogeneous substrates, and full modelling of the phenomenon would require a description of the population of different substrates with different contact angles.

1(b)

Draw lines from central lattice to all nearby lattice points. Identify midpoints of each of these lines and construct perpendicular bisectors. The smallest area enclosed by these bisectors is the first Brillouin zone.

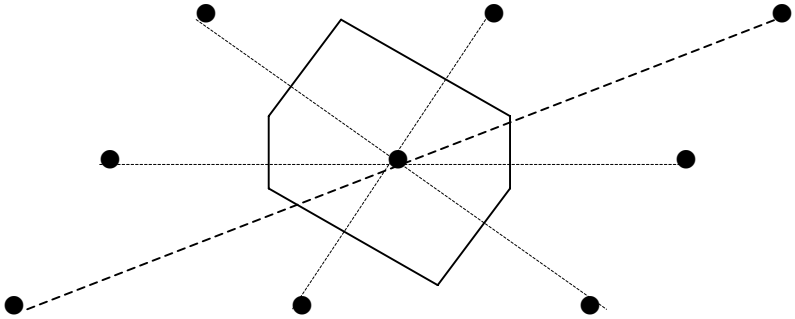

The first Brillouin zone is a primitive unit cell of the lattice and will be equal in area to the primitive unit cell defining the basic repeat unit of the pattern, i.e. a parallelogram. Therefore A = $|\mathbf{a}\times\mathbf{b}|$ = ab sinγ.

1(c)

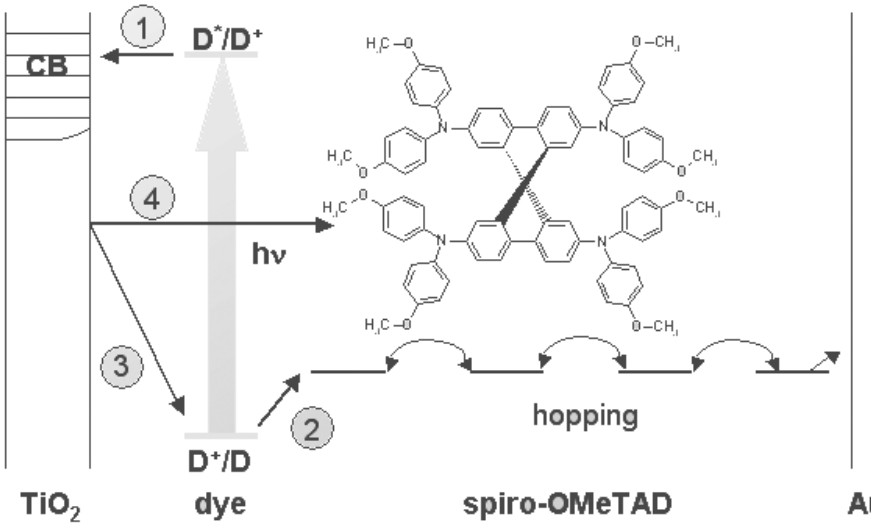

1. Electron injection from the exited state of dye into conduction band of TiO_2
2. Hole transfer from photoexited dye to orgainc hole transporter
3. Competition with recapture of injected electron by oxidized dye
4. Recombination of electrons in TiO_2 and holes in hole-transporter

1(d)

The advantages are that the enthalpy of mixing function need not be symmetric about $x = 0.5$, and can take on complex shapes depending on the number of terms in the polynomial. For $j = 0$, we get the term $x_A x_B L_{AB,0}$ which is familiar in regular solution theory, where the coefficient $L_{AB,0}$ is independent of chemical composition, and to a first approximation describes the interaction between components A and B. When $L_{AB,0} = 0$, the enthalpy of interaction between A and B is zero, and the mixture is referred to as an ideal solution.

1(e)

The following is by no means an exhaustive list:

- Vectors are well represented by one-dimensional arrays; the array corresponds to the vector as a whole, its elements to the individual vector components.
- Similarly, matrices are well represented by two-dimensional arrays, and in general an array with *n* dimensions may represent a tensor of rank *n*.
- Arrays are useful for holding interim results of numerical calculations; for example, in root-finding (numerically solving the equation $f(x) = 0$), an array could be used to store the successive values of x.
- Arrays can store (x, y) coordinates (such as for use by a plotting package). Data that could be printed in a table, or entered on a spreadsheet, can well be represented by a two-dimensional array.
- An array can often be used conveniently for workspace during a calculation, without the need to declare large numbers of individual variables. An array may be used to allocate a certain amount of memory for the program's use.

1(f)

Metals: generally any mode that absorbs energy: lattice vibrations (phonons), magnetic order-disorder, and electrons. However, electrons contribute very little since the Pauli exclusion principle prevents all but the ones located in a region kT of the Fermi level from participating in the energy absorption processes. There are extra degrees of freedom for polymers: chain curling and uncurling, molecular rotations and other vibration modes.

1(g)

Can either start with Maxwell relation $\mathrm{d}G = -S\mathrm{d}T + V\mathrm{d}p$, or derive this from definitions, $\mathrm{d}U = T\mathrm{d}S - p\mathrm{d}V$ and $G = U - TS + pV$

$$\therefore \mathrm{d}G = \mathrm{d}U - T\mathrm{d}S - S\mathrm{d}T + p\mathrm{d}V + V\mathrm{d}p$$
$$= (T\mathrm{d}S - p\mathrm{d}V) - T\mathrm{d}S - S\mathrm{d}T + p\mathrm{d}V + V\mathrm{d}p$$
$$= -S\mathrm{d}T + V\mathrm{d}p$$

To verify that G is a function of state, need to show that $\mathrm{d}G$ is exact, i.e.:

$$\left(\frac{\partial S}{\partial p}\right)_T = -\left(\frac{\partial V}{\partial T}\right)_p \qquad (*)$$

Consider the form of $\mathrm{d}G$ at constant T:

$$\mathrm{d}G = V\mathrm{d}p \Rightarrow \left(\frac{\partial G}{\partial p}\right)_T = V \qquad (**)$$

Consider the form of $\mathrm{d}G$ at constant p:

$$\mathrm{d}G = -S\mathrm{d}T \Rightarrow \left(\frac{\partial G}{\partial T}\right)_p = -S \qquad (***)$$

Differentiating (**) with respect to p at constant T and (***) with respect to T at constant p, we obtain:

$$\frac{\partial^2 G}{\partial p \partial T} = \left(\frac{\partial V}{\partial T}\right)_p = -\left(\frac{\partial S}{\partial p}\right)_T$$

which is just (*), so $\mathrm{d}G$ is exact and G is a function of state.

The Gibbs free energy G of a state cannot be directly calculated from a straightforward isothermal-isobaric (NpT) simulation by averaging over configurations, because the system will always adjust its state so as to minimise the free energy in equilibrium. Another way of saying this is that G is a thermal quantity, i.e. related to phase space volume of state, rather than mechanical quantity like energy or enthalpy.

1(h)

Grains are defined by "spins" which are mapped onto a fixed lattice. Lines (or planes in 3-D) separating regions of different spin define the grain boundaries. An example in 2-D is shown below (in this case the number of spins, Q, equals 9).

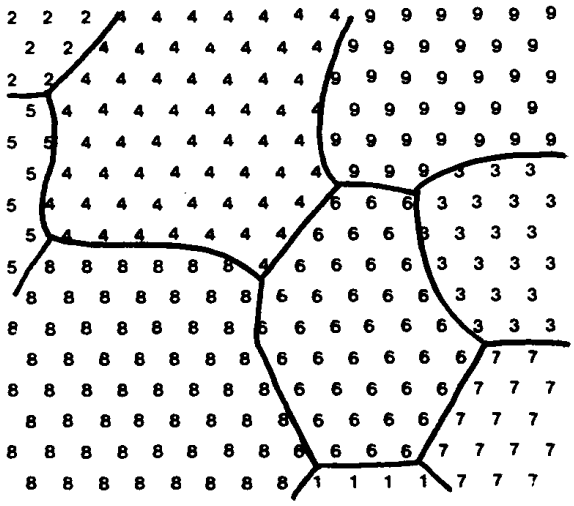

Fig. 1. Sample microstructure on a triangular lattice where the integers denote orientation and the lines represent grain boundaries.

Sites interact via a nearest neighbour potential: $H = -J\sum\left(\delta_{S_i S_j} - 1\right)$ where $1 \leq S_i \leq Q$ and $\delta_{S_i S_j} = 1$ if $S_i = S_j$ (or 0 otherwise) and J is a positive constant.

The system is allowed to evolve using stochastic dynamics (Monte Carlo). The spins are allowed to make transitions at random. Transition probabilities are computed from the Boltzmann factor at a given temperature. Transitions are accepted or rejected by comparing the Boltzmann factor to a randomly generated number between 0 and 1. Successful transitions near boundaries correspond to grain boundary migration.

1(i)

When conducting experiments, the *noise* results in a different output for the same set of inputs when the experiment is repeated. This is because there are variables that are not controlled so their influence is not included in the analysis.

The *uncertainty* of modelling deals with an entirely different problem; there many exist many mathematical functions which adequately represent the same set of empirical data but which behave differently in extrapolation. The spread of these different functions when making predictions is the required uncertainty. This spread will be greater when making large extrapolations so, in contrast to the noise, it is a variable uncertainty.

1(j)

The following points should be included in the answer:

- The discretisation at the location of the heat source must be sufficient to ensure that the energy deposited into the model is equal to that deposited in reality.
- The form of the heat source is important and the mesh should be sufficiently fine to capture this.
- The weld path for most weld analyses are long compared to the heat source dimension.
- For an ellipsoidal heat source a minimum of 4 quadratic elements or 2 cubic elements are required across each axis of the heat source.
- Where the symmetry of the component permits, analyses may be performed in the reference frame of the heat source. This allows the transient, steady-state temperature field to be calculated in a single step rather than in a step-wise fashion. Such analyses may be performed with meshes that possess a high level of mesh discretisation only around the heat source itself.
- Where analyses need to be conducted in the reference frame of the material (Lagrangian analyses) the fine level of mesh discretisation would be required along the entire path of the weld. This is likely to lead to a very considerable number of elements in the model and hence also, considerable solution times. To minimize the number of elements required in such analyses, the region in which a high degree of refinement is maintained should be minimized. The number of elements required for such models can be minimized through use of biased, graded, or adaptive remeshing schemes.

Biased mesh. These meshes employ a variation in the element size in one or more dimensions so that the required discretisation is achieved around the heat source. However, meshes of this type generate elements far from the heat source with large aspect ratios. The distortion of such elements may lead to numerical difficulties and should be avoided.

Graded mesh. By incorporating layers of triangular prismatic, distorted cuboidal or special grading elements, the element size away from the weld can be increased in more than one dimension. Whilst offering improvements over biased meshes, these meshes still result in a considerable number of elements along the weld path.

Adaptive mesh. By incorporating mesh modification strategies (refinement and de-refinement), a region with high local refinement can be made to follow the heat source. This alleviates the need to mesh the entire weld path with small elements whilst ensuring that the high thermal and stress gradients calculated in the vicinity of the heat source are accurately modelled over the entire length of the weld path.

SECTION B

2.

Fermi surfaces are surfaces of constant energy in *k*-space corresponding to the highest occupied electron energy level. Only metals have Fermi surfaces since they do not have band gaps. Due to anisotropy in the band structure the Fermi surface can be quite irregular, distorted and fragmented. The physical significance of the Fermi surface is mainly related to transport properties, although optical and magnetic properties are also influenced. In an applied electric field it is the electrons on the Fermi surface that move and contribute to electrical conductivity. The conductivity is directly proportional to the density of electrons on the Fermi surface. In an applied electric and magnetic field the electrons can perform various closed and open orbits around the Fermi surface.

[30%]

The Fermi surface for free electrons is spherical. Consider a cubic box of side L, volume V, containing N free electrons. By solving the free electron wave equation it can be shown that the allowed wave vectors of the electrons are quantized and fall on a grid in k-space of size $2\pi/L$. So in 3-D the volume per *k*-point is $\left(\frac{2\pi}{L}\right)^3 = \frac{(2\pi)^3}{V}$.

Therefore the volume of the Fermi sphere is

$$\frac{1}{2} N \frac{(2\pi)^3}{V}$$

The factor of one-half comes from the Pauli exclusion principle, which says that 2 electrons can occupy each energy level. Thus

$$\frac{1}{2} N \frac{(2\pi)^3}{V} = \frac{4}{3}\pi k_F^3$$

where k_F is the radius of the Fermi sphere corresponding to the Fermi energy. Therefore

$k_F = \left(3\pi^2 n\right)^{1/3}$ where $n = N/V$, the electron density.

[30%]

For copper, $k_F = \left(3\pi^2 \frac{4}{a^3}\right)^{1/3} = 1.365 \times 10^{10}\,\mathrm{m}^{-1}$, since there are 4 atoms (and hence 4 electrons) per unit volume in the fcc structure.

The Fermi surface occupies half the volume of the first Brillouin zone since the metal is monovalent (odd number of valence electrons per primitive unit cell).

[20%]

The Fermi surface of copper exhibits "necks" which just make contact with the 8 {111} boundaries of the first Brillouin zone. These are the boundaries that are closest to the centre of the zone. Hence the electron-ion interaction is strongest along <111> directions causing the free-electron Fermi sphere to distort.

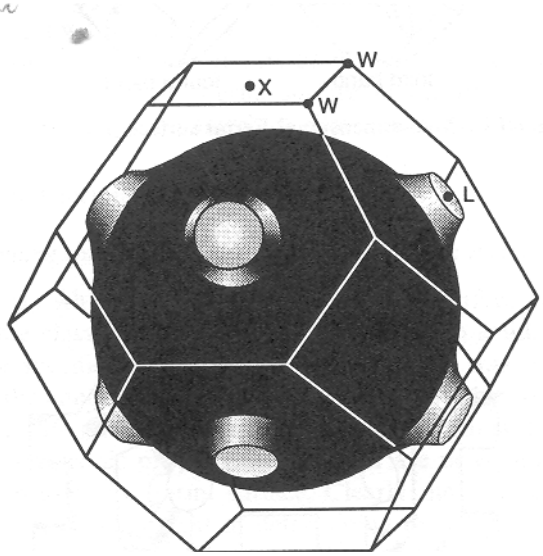

[20%]

3.

The flux may be written as a function $J\{X\}$ of the force X using a Taylor expansion about $X = 0$

$$J\{X\} = J\{0\} + J'\{0\}\frac{X}{1!} + J''\{0\}\frac{X^2}{2!} + \ldots$$

Note that $J\{0\} = 0$ since the flux is zero at equilibrium. If higher order terms are neglected, then we see that

$$J \propto X$$

The approximation lies in neglecting higher order terms. This becomes clear in the interface velocity in the subsequent part of the question.

[40%]

Consider the transfer of atoms across a grain boundary in a pure metal over a barrier of height G^*. The probability of forward jumps (which lead to a reduction in free energy) is given by

$$p_f = \exp\{-G^*/kT\}$$

whereas that of reverse jumps is:

$$p_r = \exp\{-(G^* + \Delta G)/kT\} = \exp\{-G^*/kT\}\exp\{-\Delta G/kT\}$$

The rate at which an interface moves is therefore given by:

$$v \propto p_f - p_r = \exp\{-G^*/kT\}\left(1 - \exp\{-\Delta G/kT\}\right)$$

[45%]

This relation is different from what we might expect from the thermodynamic theory of irreversible processes. However, for small ΔG, i.e. for small deviations from equilibrium, consistency is regained. In such as case, $\exp\{-\Delta G/kT\} \cong 1 - \Delta G/kT$, and hence

$$v \propto \exp\{-G^*/kT\}\left(\Delta G/kT\right)$$

[15%]

4.

(a) Properties that need to be considered are:

- weight and density (pole needs to be light and also float);
- stiffness and yield strength;
- fracture toughness;
- cost.

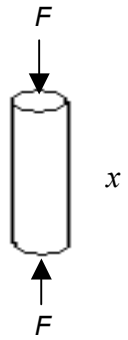

(b) Possible failure modes are:

- plastic yielding if metallic pole;
- brittle failure;
- Euler buckling.

[20%]

Performance index: mass m = volume × density = $x\pi r^2\rho$

$$\text{pole will buckle if } F > \frac{C\,\pi^2\,E\,I}{x^2}$$

Length of punt pole is not a variable but, within limits, radius r can be and so is treated as a "free variable". Hence r can be eliminated between the two equations, and so

$$F_{crit} = \frac{C\,\pi^2\,E\,I}{x^2} = \frac{C\,\pi^3\,E\,r^4}{4x^2} = \frac{C\,\pi\,E\,m^2}{4x^4\rho^2}$$

Rearranging gives : $m = \frac{2}{\sqrt{\pi}} \quad \frac{x^2}{\sqrt{C}} \quad F_{\text{crit}}^{0.5} \quad \left[\frac{\rho}{E^{0.5}}\right]$

Hence can minimise mass if choose materials with largest value of

$$\left[\frac{E^{0.5}}{\rho}\right]$$

Using selection chart of modulus versus density, possible materials are:

wood: good cheap and traditional choice which floats;

CFRP / CGRP: would last "indefinitely" but considerably more expensive, tougher;

aluminium: possible but would not float if solid – as specified in questions.

All three materials are reasonably easy to fabricate and also are resistant to degradation.

Can also check toughness using second chart and all three materials are good choices.

[60%]

Improvements:

Need to consider shape and tubular construction would result in lower weight and greater stiffness.

This would favour use of tubular aluminium – easy to fabricate, cheaper as now less material and also can fill with foam so that pole will float.

[20%]

5.

$$U(x)=\begin{cases}\alpha A x^2 & x<0\\ \alpha\left[1-\cos\left(2\pi x\right)\right] & 0\le x\le 1\\ \alpha A\left(x-1\right)^2 & x>1\end{cases}$$

$$F(x)=\frac{\mathrm{d}U}{\mathrm{d}x}=\begin{cases}2\alpha A x & x<0\\ 2\pi\alpha\sin\left(2\pi x\right) & 0\le x\le 1\\ 2\alpha A\left(x-1\right) & x>1\end{cases}$$

$$\frac{\mathrm{d}F}{\mathrm{d}x}=\begin{cases}2\alpha A & x<0\\ \left(2\pi\right)^2\alpha\cos\left(2\pi x\right) & 0\le x\le 1\\ 2\alpha A & x>1\end{cases}$$

Hence, equating $\frac{\mathrm{d}F}{\mathrm{d}x}$ at $x = 0$ and $x = 1$ for continuity, we obtain:

$2\alpha A=\left(2\pi\right)^2\alpha\Rightarrow A=2\pi^2$

Check that this gives continuity at $x = 0$ and $x = 1$ for U and F:

$U(0)$ $\quad 0 = 0$ OK
$F(0)$ $\quad 0 = 0$ OK

$U(1)$ $\quad 0 = 0$ OK
$F(1)$ $\quad 0 = 0$ OK

Potential shown below for $\alpha = 1$, with three stationary points at $x = 0$, 1 (minima) and $x = 0.5$ (maximum). Value of $U(0.5) = \alpha$

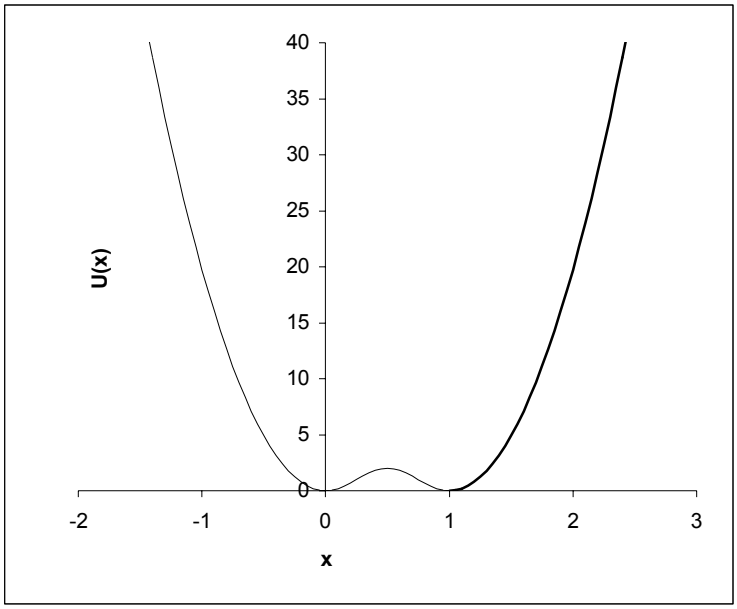

[50%]

MD solves Newton's equations of motion for system, with forces calculated from above expressions. Temperature control achieved using Berendsen or Nosé-Hoover thermostat, as described in lectures.

[30%]

As temperature is increased from $T = 0$, particle is initially trapped in minimum around $x = 0$. Once temperature reaches $T \cong \alpha / k_B$, then significant crossing of the barrier at $x = 0.5$ begins to occur. At temperatures $T \gg \alpha / k_B$, the behaviour of particle looks very similar to one confined in quadratic potential well.

[20%]

6.

When the pure phases α and β are in equilibrium, their Gibbs free energy are equal, $G^{\alpha} = G^{\beta}$.

[10%]

Consider α phase consisting of two components A and B. The free energy of α is a function of the mole fractions $(1-x)$ and x of A and B, respectively:

$$G^{\alpha} = (1-x)\mu_A + x\mu_B$$

where μ_A represents the mean free energy of a mole of A atoms in α phase. The term μ is called the chemical potential of A. Thus, the free energy of a phase is simply the weighted mean of the free energies (chemical potentials) of its component atoms.

Consider now the coexistence of two phases α and γ in the binary alloy. They will only be in equilibrium with each other if the A atoms in α have the same free energy as the A atoms in γ, and if the same is true for the B atoms:

$$\mu_A^{\alpha} = \mu_A^{\gamma}$$
$$\mu_B^{\alpha} = \mu_B^{\gamma}$$

The condition that the chemical potential of each species of atom must be the same in all phases at equilibrium is general and justifies the common tangent construction as illustrated in the figure below.

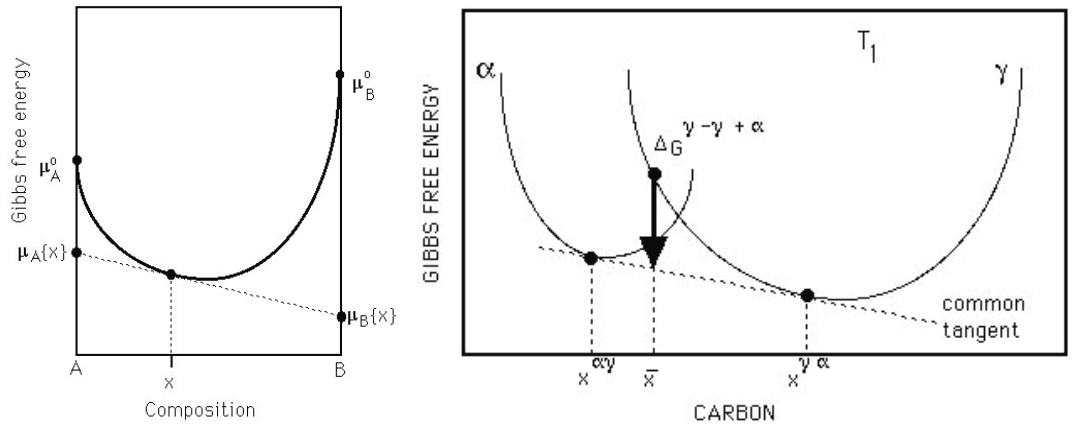

Notice that in the figure above, the common tangent gives identical intercepts for both α and γ at $x = 0$ and 1.

[25%]

The binding energy defined relative to infinitely separated atoms, before mixing, is

$$E = \frac{1}{2} zN\left[(1-x)(-2\varepsilon_{AA}) + x(-2\varepsilon_{BB})\right]$$

since the binding energy per pair of atoms is $-2\varepsilon_{ij}$, and $\frac{1}{2}zN$ is the number of bonds.

[25%]

To do what follows requires a major assumption that the atoms are randomly disposed. This assumption can alternatively be expressed by saying that the temperature is high enough for entropy effects to overwhelm any enthalpy terms. For a binary $(A-B)$ solution, the numbers of the different kinds of bonds can be calculated using simple probability theory. Given a concentration x of B and a lattice coordination number z, and the fact that the probability of finding a B atom in a random solution is x, it follows that

$$N_{AA} = z\,\tfrac{1}{2}N(1-x)^2$$
$$N_{BB} = z\,\tfrac{1}{2}Nx^2$$
$$N_{AB} + N_{BA} = zNx(1-x)$$

where N_{AB} represents both A–B and B–A bonds which cannot be distinguished. N is the total number of atoms. Notice that the unlike bonds A–B and B–A cannot be distinguished and hence have been consolidated. After mixing, the corresponding energy is given by:

$$E_{mix} = \frac{1}{2} zN\left[(1-x)^2(-2\varepsilon_{AA}) + x^2(-2\varepsilon_{BB}) + 2x(1-x)(-2\varepsilon_{AB})\right]$$

where the factor of two in the last term is to count both A–B and B–A bonds.

[25%]

Therefore, the change in energy due to mixing is given by

$$\begin{aligned}\Delta E &= E_{\text{mix}} - E \\ &= -zN\left[(1-x)^2(\varepsilon_{AA}) + x^2(\varepsilon_{BB}) + 2x(1-x)(\varepsilon_{AB}) - (1-x)(\varepsilon_{AA}) - x(\varepsilon_{BB})\right] \\ &= -zN\left[-x(1-x)(\varepsilon_{AA}) - x(1-x)(\varepsilon_{BB}) + x(1-x)(2\varepsilon_{AB})\right] \\ &= zNx(1-x)\omega\end{aligned}$$

where $\omega = \varepsilon_{AA} + \varepsilon_{BB} - 2\varepsilon_{AB}$.

[15%]

7.

Thermodynamic effect of grain size — Grain boundaries are defects and raise the free energy of the solid. In normal polycrystalline materials (i.e. with grain diameter > 100 nm or so) the effect is weak because such a small fraction of the atoms in the material lie in grain-boundary regions. The effects are seen mainly in nanocrystalline materials. In principle all phase equilibria are affected. The example most likely to be discussed is reduction of the melting temperature of the solid.

[5%]

Elastic — The Young modulus is one possible measure of stiffness. Stiffness is lowered in grain-boundary regions. The effect is so weak however, that the Young modulus is normally taken to be an *intrinsic* property (not affected by *microstructure*). Measurable reduction in the modulus is seen in nanocrystalline materials.

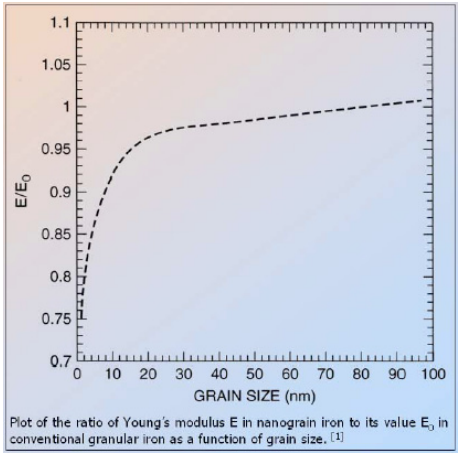

Plot of the ratio of Young's modulus E in nanograin iron to its value E_0 in conventional granular iron as a function of grain size. [1]

[10%]

Plastic — Grain boundaries are barriers to the transmission of dislocations from one grain to another. The yield stress or hardness of a material (in particular a metal, since these are the important category of material showing dislocation-mediated plastic flow) increases as the grain size is decreased. This is a strong effect and the yield stress is considered an *extrinsic* property (affected by *microstructure*). The effect is described by the *Hall-Petch relationship*:

$$\sigma_y = \sigma_{y,0} + kd^{-0.5}$$

where σ_y is the yield stress, $\sigma_{y,0}$ is the limiting value of σ_y at large grain size, k is a constant and d is the average grain diameter. (Some may note that this relationship begins to break down in nanocrystalline materials, with a saturation in yield stress.)

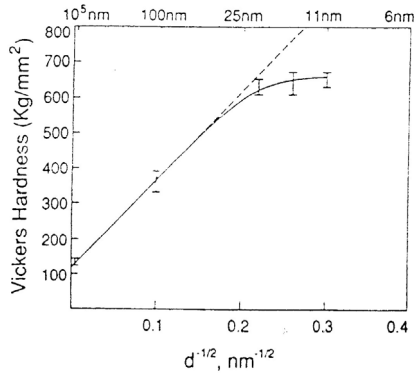

For electrodeposited nanocrystalline nickel

[10%]

Optical — In an intrinsically transparent material, which is optically anisotropic, grain boundaries can scatter light. This can render the material translucent or opaque. Transparency can be restored by reducing the grain size below the wavelength of light. (Practically important cases include transparency for wavelengths outside the visible range.)

[5%]

Magnetic — Change of magnetization involves migration of domain walls. Domain walls can be pinned by microstructural features. Greater pinning makes a harder magnet, characterized as increased *coercivity*. As the grain size of a polycrystalline magnet is decreased, the coercivity increases roughly as $1/d$. This is a strong effect, changing the coercivity by roughly four orders of magnitude, covering both soft and hard magnets. As the grain-size is reduced in the range 100 down to 10 nm, however, the scale of the microstructure falls below the domain-wall width and the pinning disappears, giving soft magnetic properties similar to those of an amorphous alloy.

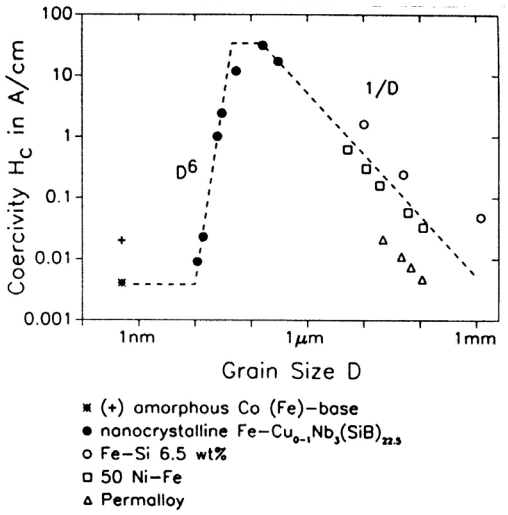

[10%]

In diffusional creep, individual grains show the same elongation as the overall sample. In superplastic flow, the grains remain equiaxed and the grain structure does not alter in its average characteristics.

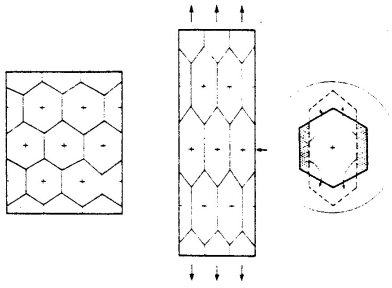

[5%]

The main mechanism of superplastic flow (the Ashby-Verrall mechanism) is local grain rearrangement by grain-boundary sliding, with the necessary diffusional accommodation.

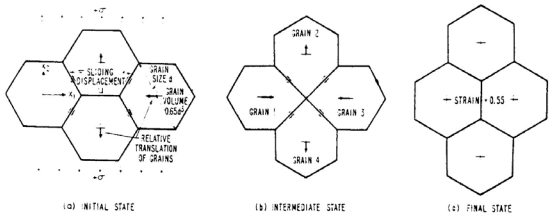

[5%]

Requirements are that the grain size should be *fine* and *stable*.

[5%]

To maintain a fine grain size (i.e. to inhibit grain growth) we need to (i) have a microstructure of two phases in roughly equal volume fractions, OR (ii) have a dispersion of fine particles to pin the boundaries.

[5%]

Nanocrystalline materials are of interest, because as the grain size is decreased the superplastic flow rate increases (at a given temperature). Equivalently, a given flow rate can be achieved at a lower temperature.

[5%]

Ceramics and intermetallics are brittle and not easy to shape by dislocation-mediated plastic flow. They are also refractory materials showing only low creep rates. For such materials superplastic flow is an attractive shaping method. For normal grain sizes, however, the flow is too slow. In nanocrystalline materials the flow is intrinsically faster and practically useful flow rates are obtained at lower temperatures.

[15%]

Assume same $\dot{\varepsilon}$, so that:

$$\left(\frac{d_1}{d_2}\right)^{2.5} = \exp\left[\frac{-Q}{R}\left(\frac{1}{T_1}-\frac{1}{T_2}\right)\right]$$

d_1 = 600 nm; d_2 = 60 nm; d_1/d_2 = 10; Q = 250 kJ mol^{-1}; R=8.314 J K^{-1} mol^{-1}; T_1 = 1473 K.

We find that T_2 = 1149 K = 876˚C — i.e. the flow temperature is reduced by 324˚C.

[20%]